# Development and performance evaluation of large-area Compton camera

Young-su Kim [a], Jae Hyeon Kim [a], Hyun Su Lee [a], Jong Hoon Park [a], Han Rim Lee [b], Chan Hyeong Kim [a*]
[a]*Dept. of Nuclear Engr., Hanyang Univ., 222 Wangsimni-ro, Seongdong-gu, Seoul 04763, Korea*
[b]*Korea Atomic Energy Research Institute, 111 Daedeok-daero 989beon-gil, Yuseong-gu Daejeon 34057, Korea*
[*]*Corresponding author: chkim@hanyang.ac.kr*

## 1. Introduction

Compton imaging is a method for imaging the location or distribution of radioactive materials emitting gamma-rays [1]. It provides the ability to detect high-energy (from several hundred keV to several MeV) gamma-rays with large field-of-view by using electronic collimation based on Compton kinematics. With this advantage, Compton cameras have been studied for various applications [2,3]. While a Compton camera provides better performance than mechanical-collimator-based imaging systems, there is still room for improvement in the detection efficiency.

To improve efficiency without degradation of image resolution of a Compton camera, we suggest to use large monolithic scintillation detectors. A monolithic scintillation detector with an array of optical light sensors has a potential to provide millimeter-order spatial resolution by applying advanced interaction position estimation algorithm, like maximum likelihood position estimation (MLPE) [4]. In this context, we developed a large-area Compton camera using monolithic scintillation detectors and evaluated its performance.

## 2. System configuration

In this section, we will describe the large-area Compton camera including the detector modules and the data acquisition system for the modules. We will also briefly explain an image reconstruction algorithm used in the experiments for performance evaluation of the developed Compton camera.

### *2.1 Detector Module*

The large-area Compton camera is composed of two large monolithic scintillation detector modules. Each module contains a detector head built by Scintitech (MA, USA) and dedicated signal processing circuits. Fig. 1 shows the detector modules composing the Compton camera.

For each detector head, we selected to use a monolithic NaI(Tl) scintillator with an array of photomultiplier tubes (PMT). The dimension of the NaI(Tl) scintillator, used in this study, is 27 cm (W) × 27 cm (H) × 2 cm (T). The scintillator is sealed by an aluminum case and a 1-cm thick optical window. The array of PMTs is optically coupled to the optical window using BC630 optical grease (Saint-Gobain, France). One of the detector heads, used for the front plane of the Compton camera, is coupled with 6 × 6 rectangular array of 36 square-shaped PMTs (XP3290, Photonis, France), while the other one used for the back plane is coupled with hexagonally arranged 22 cylindrical PMTs (R6231-01, Hamamatsu, Japan).

The signals from every channel need to be handled individually to apply the advanced interaction position estimation algorithms. Since there are too many signal channels for each detector to directly control them, multiplexer-based signal processing circuits were developed. In the beginning of the circuit, a trigger signal is generated when the sum of the signals is over the threshold level. As soon as the trigger signal is generated, the circuit outputs 8-to-1 multiplexed signals of peak voltages of each channel with a transition time of 1 μs per channel. The total signal processing time for one trigger is about 10 μs. With the developed signal processing circuits, the number of signal channels is reduced by one-eighth, i.e., five channels for 36 PMTs and three channels for 22 PMTs.

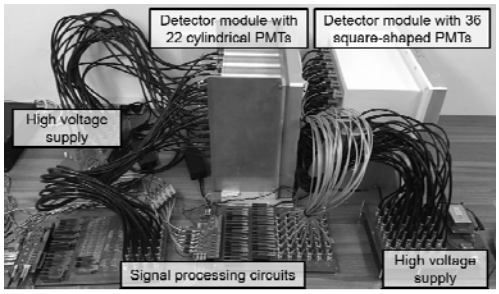


Fig. 1. Detector modules composing the large-area Compton camera.

### *2.2 Data acquisition system*

The data acquisition system of large-area Compton camera mainly has three functions: selection of coincided events, decomposition of the multiplexed data, and estimation of deposited energy and interacted position.

A coincidence check circuit was developed to select coincident events between two detector modules. The circuit receives trigger signals from the two detector modules, and then generates coincidence signal only when the time difference between two triggers is less than the time window of 200 ns.

Once the coincidence trigger is generated, the multiplexed signals from the two detector modules are transmitted to a FlexRIO board (National Instruments,

TX, USA) which is based on a field programmable gate array (FPGA). In the FlexRIO, the multiplexed signals are de-multiplexed into each channels, and then finally the voltage values of 58 (36+22) channels per trigger are transferred to a personal computer by a PXI-e line.

The deposited energy and interaction position in each detector module are calculated in the personal computer. Deposited energy was calculated based on the proportionality to sum voltage of all channels of a detector module. The interaction position was estimated by MLPE based on a scaled-Poisson distribution [4] considering that electrical noise of PMTs is negligible. For the pre-process of MLPE, a look-up table was generated by Geant4 simulation, which contains the mean detector response for each reference position of 1-mm grid pattern.

### *2.3 Image reconstruction*

In the evaluation experiments, the list-mode maximum-likelihood expectation maximization (LMMLEM) algorithm [5] was used to reconstruct Compton image from the energy and position data. A total number of iterations to perform LMMLEM algorithm was empirically chosen as 50 iterations.

Two kinds of image space were used in this study: a hemispherical surface and a three-dimensional Cartesian coordinate space. In the case of the hemispherical surface, the coordinate system was defined such that a source centered directly in front of the Compton camera has angular coordinates (0°, 0°). The whole image space was from −90° to 90° in azimuthal angle and from −90° to 90° in polar angle with 0.5° bin for each axis. For the Cartesian coordinate system, we defined the front direction of Compton camera as +z direction. In this case, the voxel size of the image space was 1 cm × 1 cm × 2 cm.

## 3. Experimental results and discussion

This paper presents results from two experiments that evaluate the performance of the large-area Compton camera. The first experiment with a $^{137}$Cs check source was used to measure the basic performance of the Compton camera such as detection efficiency and image resolution. The other experiment with the $^{137}$Cs and $^{60}$Co check sources was performed to show the ability of the developed Compton camera to distinguish multiple sources in three-dimensional space by a single measurement. In the context of this work, a data that the sum of deposited energy is within the energy window is referred to as a valid event.

### *3.1 Imaging $^{137}$Cs point source at the axis*

A 16.1-μCi $^{137}$Cs point source (662 keV gamma-ray) was measured with the Compton camera for 30 seconds. The $^{137}$Cs had angular coordinates of (0°, 0°) and was located at 100 cm from the center of the Compton camera. The exposure rate at the center of the Compton camera was 0.048 μSv/h which is nearly half of the natural background level. In this experiment a total of 276 valid events were detected with an energy window of 600–720 keV, which means the absolute efficiency is $1.8\times10^{-5}$. Fig. 2 shows the sum energy spectrum and the reconstructed image. The energy resolution of the sum spectrum for 662 keV was 10.5%. In the reconstructed image, the $^{137}$Cs created a hot-spot occupying the pixel (−1.0°, 1.5°) with the resolution of 4.10° in full width at half maximum (FWHM).

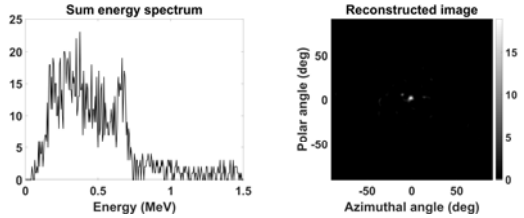


Fig. 2. Sum energy spectrum (left) and reconstructed image (right) in the experiment with the $^{137}$Cs placed at (0°, 0°).

### *3.2 Imaging two point sources*

$^{137}$Cs and $^{60}$Co point sources were measured simultaneously with the large-area Compton camera. The $^{137}$Cs source which produces 662 keV gamma-rays was located at the Cartesian coordinates (20, 0, 50) cm. The $^{60}$Co which produces 1.17 MeV and 1.33 MeV gamma-rays was located at (0, −20, 50) cm. In this experiment, the energy window for the $^{60}$Co was 1.0–1.4 MeV. The $^{137}$Cs had an activity of 8.10 μCi and the $^{60}$Co had an activity of 4.33 μCi. These activities corresponded to an approximate exposure rate of 0.081 μSv/h from the $^{137}$Cs and 0.173 μSv/h from the $^{60}$Co. The reconstructed images for each energy window are shown in Fig. 3 and Fig. 4. In these images, we see distinct hot-spots for the $^{137}$Cs and the $^{60}$Co in pixel (21, −2, 50) cm and (−1, −20, 48) cm, respectively. For the $^{137}$Cs, image resolution was evaluated as (3.4, 3.3, 5.7) cm in FWHM. For the $^{60}$Co, image resolution was (2.6, 3.7, 7.1) cm in FWHM.

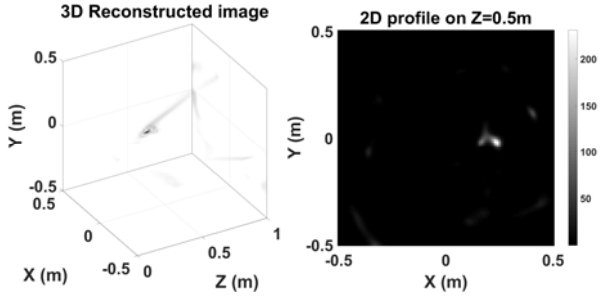


Fig. 3. Three-dimensional reconstructed image (left) and its two-dimensional profile on Z = 0.5 m plane in the two sources experiment with the energy window for the $^{137}$Cs.

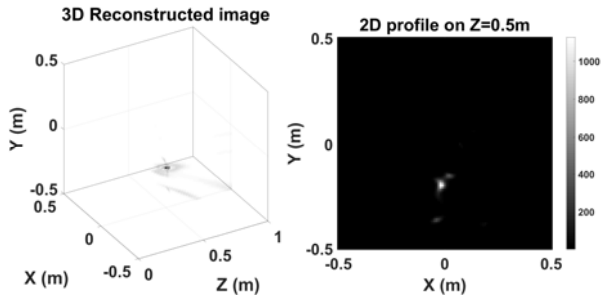


Fig. 4. Three-dimensional reconstructed image (left) and its two-dimensional profile on Z = 0.5 m plane (right) in the two sources experiment with the energy window for the $^{60}$Co.

### *3.3 Discussion*

In the first experiment with single $^{137}$Cs source, we were able to demonstrate the developed large-area Compton camera could achieve the excellent performance in detection efficiency. There was also no degradation of image resolution in enlarging detector size; the image resolution of 4.10° FWHM is similar to or better than those of small-sized Compton cameras.

The experiment with the $^{137}$Cs and $^{60}$Co showed that the developed Compton camera can distinguish multiple hot-spots clearly. We also found that the large-area Compton camera is able to provide three-dimensional images, even for the sources placed farther than 50 cm, without any auxiliary equipment or multiple measurements at different positions. It is known that a Compton camera can theoretically provide three dimensional images. However, as increase of the distance between a source and a Compton camera, uncertainty of the estimated distance is also rapidly increased. It is mainly because the Compton cones overlap following the direction of the source location, when the source distance is significantly farther than the variation of apex position of the cones (area of the scatter detector). Due to this, for most small-sized Compton cameras, 3-D detectable region is generally smaller than about 10-cm radius, which is hardly applicable to practical application. On the other hand, the developed Compton camera has a large-size scatter detector with excellent spatial resolution, which concludes the 3-D detectable region of the large-area Compton camera could be enlarged enough to be applied to real world problems.

## 4. Conclusions

The large-area Compton camera was developed and its performance was evaluated with various experiments. A novel feature of this work is the use of large monolithic scintillation detectors for enlargement of the Compton camera. In doing so, the efficiency of the Compton camera has been dramatically improved without degradation of image resolution. Moreover, the experiment in this work demonstrated that the large-area Compton camera could define the three-dimensional location of the sources for the distance of nearly 50 cm.

Overall, the results of this study serve to demonstrate the great potential of the large-area Compton camera based on large monolithic scintillation detector. In the near future, we will change the cylindrical-PMT-based detector module into the square-shaped-PMT based module to improve the performance. With a new detector module and a system optimization study, the performance of the large-area Compton camera could be improved.

## REFERENCES

[1] R. W. Todd, J. M. Nightingale, and D. B. Everett, A Proposed Gamma Camera, Nature, Vol. 291, pp. 132-134, 1974.
[2] C. G. Wahl, W. R. Kaye, W. Wang, F. Zhang, J. M. Jaworski, A. King, Y. A. Boucher, and Z. He, The Polaris-H Imaging Spectrometer, Nucl. Instruments Methods Phys. Res. Sect. A Accel. Spectrometers, Detect. Assoc. Equip., Vol. 784, pp. 377–381, 2015.
[3] A. Kishimoto, J. Kataoka, T. Nishiyama, T. Fujita, K. Takeuchi, H. Okochi, H. Ogata, H. Kuroshima, S. Ohsuka, S. Nakamura, M. Hirayanagi, S. Adachi, T. Uchiyama, and H. Suzuki, Performance and Field Tests of a Handheld Compton Camera Using 3-D Position-sensitive Scintillators Coupled to Multi-pixel Photon Counter Arrays, J. Instrum., Vol. 9, No. 11, pp. P11025–P11025, 2014.
[4] L. R. Furenlid, J. Y. Hesterman, and H. H. Barrett, Fast Maximum-likelihood Estimation Methods for Scintillation Cameras and Other Optical Sensors, Proc SPIE Int Soc Opt Eng, Vol. 6707, pp. 67070N-1, 2007.
[5] X. Lojacono, Image Reconstruction for Compton Camera with Application to Hadrontherapy, Ph. D. thesis, 2014.